Engineering Geology 174 (2014) 73–86

Contents lists available at ScienceDirect

Engineering Geology

journal homepage: www.elsevier.com/locate/enggeo

Geoelectrical prospecting of glauberite deposits in the Ebro basin (Spain)

Ander Guinea [a,b,*], Elisabet Playà [b], Lluís Rivero [b], Josep Maria Salvany [c]

[a] National Center of Groundwater Research and Training, UNSW Australia, 110 King Street, 2093, Manly Vale, NSW, Australia
[b] Departament de Geoquímica, Petrologia i Prospecció Geològica, Facultat de Geologia, Universitat de Barcelona, Martí i Franquès s/n, 08028 Barcelona, Spain
[c] Departament d'Enginyeria del Terreny, Cartogràfica i Geofísica, Universitat Politècnica de Catalunya, Jordi Girona 31, 08034 Barcelona, Spain

ARTICLE INFO

Article history:
Received 1 November 2012
Received in revised form 10 March 2014
Accepted 15 March 2014
Available online 25 March 2014

Keywords:
Glauberite
Gypsum
Electrical resistivity tomography
Karst

ABSTRACT

Glauberite ($Na_2Ca[SO_4]_2$) is an evaporitic mineral which is used in the industries of detergents, paper, glass, pharmacy, etc. Glauberite rocks are seldom found cropping out because they are very sensitive to weathering processes; for this reason their prospection is conducted by means of boreholes. Nowadays, geophysical techniques are not used to support the characterization of glauberite deposits due to the lack of knowledge of their physical properties.

In this study geoelectrical methods are proposed as alternative techniques in the early stages of glauberite prospecting. Several glauberite units have been studied in different parts of the Ebro basin (Spain) by means of electrical resistivity tomography sections. The electrical resistivity range showed by glauberite deposits has been found to be low (10–100 Ω·m) when the matrix component (clay and microcrystalline carbonates) is above 45% of the bulk composition of the rock. This type of rocks has been studied in Montes de Torrero (Zaragoza) and is the most common glauberite deposit case. Besides matrix-rich glauberite rocks, an exceptional case of a pure glauberite layer has been studied in Alcanadre (La Rioja). From this site, it has been estimated that deposits with glauberite crystal fraction close to 100% show a resistivity range of at least 3×10^3 Ω·m.

Using this extreme value as reference, the Hashin–Shtrikman bounds have been calculated for glauberite rocks considering that they are constituted of four phases (glauberite, gypsum, anhydrite and matrix). When the matrix fraction represents 45% or more of the bulk rock, the resistivity range will be that of the lower Hashin–Shtrikman bound, which is similar for any combination of sulfate (glauberite, gypsum and/or anhydrite) composition; hence, it can be considered as a two-phase system (matrix and sulfate). For rocks with less than 30% of matrix fraction, the upper Hashin–Shtrikman bound trend must be considered; however, the resistivity values overlap, making it impossible to establish a classification. Between 30 and 45% of matrix fraction, there is a transitional domain.

Additionally, some theoretical models representing the most common structures in sulfate rocks have been elaborated in order to help in the interpretation of the inverted resistivity images obtained from the field data. Some artifacts generated by the complexity of the resistivity distribution of the terrain have been identified in both data sets.

1. Introduction

Glauberite is a sodium and calcium sulfate ($Na_2Ca[SO_4]_2$) evaporitic mineral. It is usually associated with other evaporitic minerals as gypsum, anhydrite, thenardite or halite, and embedded within a clayey, marly or carbonatic (dolomite or magnesite) matrix, but their mineral association and relative abundance can strongly vary from one glauberite deposit to another (Salvany, 2009). Glauberite rocks are currently used for industrial purposes; the main producing countries are Mexico, Spain, USA, Canada and Iran (Garret, 2001). Glauberite is mainly used as a component in the powdered detergent for washing machines, but it is also exploited in the industries of paper, glass, pharmacy, textile, for the synthesis of enzymes (in the elaboration of wine), etc.

Glauberite rocks rarely outcrop because they can be easily dissolved and/or transformed into secondary gypsum during exhumation, conducted by meteoric waters. Hence, the prospection of glauberite units has to be made by means of mechanic boreholes, which are expensive and give only local information. Nowadays geophysical methods are not applied to the prospection of these deposits due to the lack of information regarding their geophysical properties; the electrical resistivity response of glauberite rocks has not been previously studied. Although no references exist on this topic, it is supposed as an initial hypothesis that the resistivity value for glauberite crystals will be higher than the one of gypsum ($CaSO_4 \cdot 2H_2O$) crystals, due to the lack of water in his crystalline structure as in the case of anhydrite ($CaSO_4$) crystals

* Corresponding author.
E-mail addresses: a.guinea@unsw.wrl.edu.au (A. Guinea), eplaya@ub.edu (E. Playà), lrivero@ub.edu (L. Rivero), josepm.salvany@upc.edu (J.M. Salvany).

http://dx.doi.org/10.1016/j.enggeo.2014.03.007
0013-7952/

(Guinea et al., 2011). Unlike the cases of glauberite and anhydrite, in the gypsum crystals the electrical current runs preferably along its water layers.

The electrical resistivity of gypsum rocks with a gypsum crystal fraction close to 100% in their composition is approximately 10^3 Ω·m (Guinea et al., 2010a), while electrical resistivity of anhydrite rocks with similar anhydrite crystal fraction in their composition is close to 10^4 Ω·m (Guinea et al., 2012). In the case of calcium sulfate rocks (rocks with gypsum and/or anhydrite plus matrix), the influence of the presence of matrix (mainly clay and microcrystalline carbonates) in the electrical resistivity has been described as critical (Guinea et al., 2010b). Hence, when the matrix content in the rock is higher than 45%, the matrix is connected at long range resulting in a percolating system. Because of this, the electrical resistivity of these rocks is dominated by the matrix component and not affected by differences in the composition of the sulfate fraction (different combinations of gypsum and anhydrite). Glauberite rocks were used to enclose large quantities of matrix so it can be considered that they will commonly be affected by this same matrix-dominance effect. Some of these matrix-rich glauberitic deposits have been studied in the Zaragoza sector of the Ebro basin. Additionally, besides glauberitic deposits in which the matrix is the dominant component, a case of an outcropping glauberite-rich layer has been studied in the western part of the Ebro basin. Likely layers are present in other glauberitic deposits, but exceptionally resist the weathering at shallow conditions.

In addition to compositional differences, the structures which are commonly found in the sulfate rocks had an effect on the resistivity distribution of the terrain. Due to the relatively high solubility of sulfate minerals, secondary porosity can be developed (Gutierrez et al., 2002; Warren, 2006). This porosity generation occurs at different degrees, from centimeter-scale tunnels to a regional karstification (Guerrero et al., 2003). In field observations, it is possible to find these structures as filled or empty karst cavities. From the geoelectrical point of view, the response of the terrain will differ greatly between both cases. In the case of filled karst, the infilling materials are generally lutites and sulfate blocks; these structures will be reflected in the geoelectrical profiles as a dramatic resistivity decrease in the area, making the sulfate layer discontinuous. In the other hand, an empty karst will display a very high-resistivity anomaly because the resistivity of the air tends to infinity. Besides the secondary-porosity structures, sulfate rocks usually display lateral variations originated during their deposition (primary structures, such as vertical and/or lateral compositional changes). These changes can be gradual or sharp and may generate resistivity variations of the sulfate layers (depending of their composition). Additionally, the original sulfate layers can be folded or faulted generating more complex structures as diapires and making the interpretation of the resistivity distribution even more difficult.

The scope of this study is to characterize the geoelectrical response of glauberite deposits, to define their range of resistivity and to evaluate the influence of accompanying minerals and their associated structures. The resistivity has been studied in several evaporitic deposits of the Ebro basin with the electrical resistivity tomography (ERT). In addition, some common structures in sulfate rocks have been modeled and their effect in the resistivity of the terrain has been analyzed in order to be compared with the performed field sections. Obtained information will improve the interpretation of resistivity data sets on this type of rocks and make ERT a useful tool for future prospecting of glauberite deposits.

2. Geological setting

Glauberite deposits are well developed in the non-marine evaporite Zaragoza Gypsum Formation infilling the Ebro basin (NE Spain), which were deposited throughout the Miocene (Fig. 1). More than 4000 m of detrital and evaporitic sediments derived from the denudation of the surrounding chains (Pyrenees and Iberian Chain) sedimented during

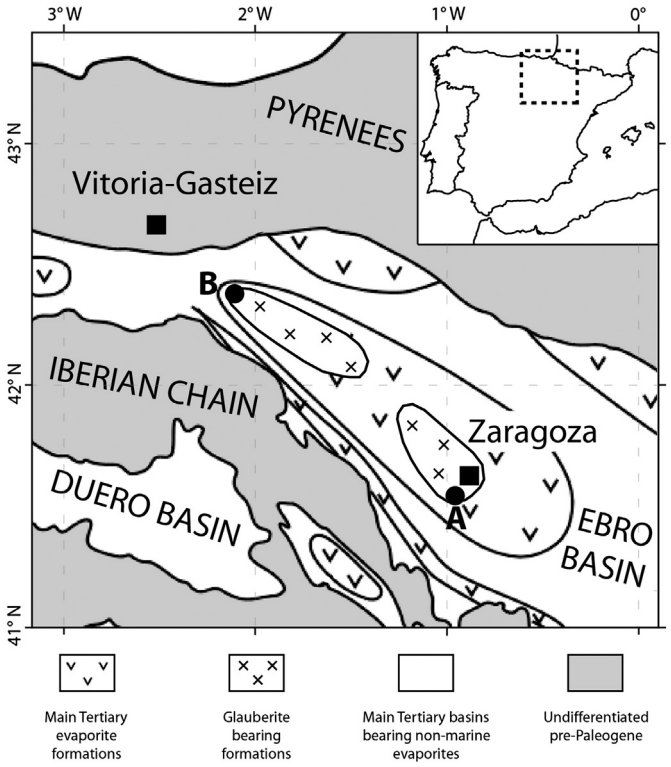

Fig. 1. Main Tertiary basins in the middle-North Spain. A and B are the two studied areas; Montes de Torrero (Zaragoza) and Alcanadre (La Rioja) sectors, respectively. Modified from Ortí et al. (2010).

the basin infilling, including thick sequences of glauberite together with gypsum, anhydrite, thenardite and halite rocks. These evaporites precipitated in several shallow lacustrine systems in the central parts of the basin, while coeval alluvial systems formed in the basin margins (Orti, 1997; Orti and Salvany, 1997). Glauberite mainly grew as interstitial fine (less than 1 mm) to large crystals (up to several centimeters) within the more distal alluvial sediments deposited around the lake or in its floor (glauberite bearing lutite or marl matrix). Less frequently, glauberite also grew as large crystals on the lake floor that were subsequently cemented by halite (glauberite without matrix) (Salvany et al., 2007). The burial processes did not significantly affect the primary structures and mineralogy of the glauberite and its associated minerals; only the gypsum was transformed into anhydrite by dehydration under the increasing pressure and temperature at depth. The current erosive period has caused the exhumation of the evaporite deposits and its weathering by the infiltration of the meteoric waters. This waters caused the partial (or locally total) dissolution of the more soluble minerals (mainly halite), and the gypsification of glauberite and anhydrite rocks. Thus, a superficial cover of secondary gypsum of several tens of meters thick (occasionally more than 100 m thick) was formed. This cover is composed of gypsum pseudomorphs after glauberite and gypsum nodules after anhydrite, all them embedded in variable amounts of fine detrital sediments. The vertical transition between the unweathered deposits, at depth, and the superficial cover is very gradual. It forms an intermediate zone several meters thick where all minerals (primary and secondary) can be mixed. Subsequent karstic structures usually characterize the upper part (generally not below 10 m of the surface) of this gypsiferous cover.

The glauberite deposits considered in this study are only a small part of the glauberite record of the Ebro basin, which is still little known. The studied glauberite deposits are found in the Alcanadre and Montes de Torrero areas, respectively in the western and central sectors of the Ebro basin (Fig. 1).

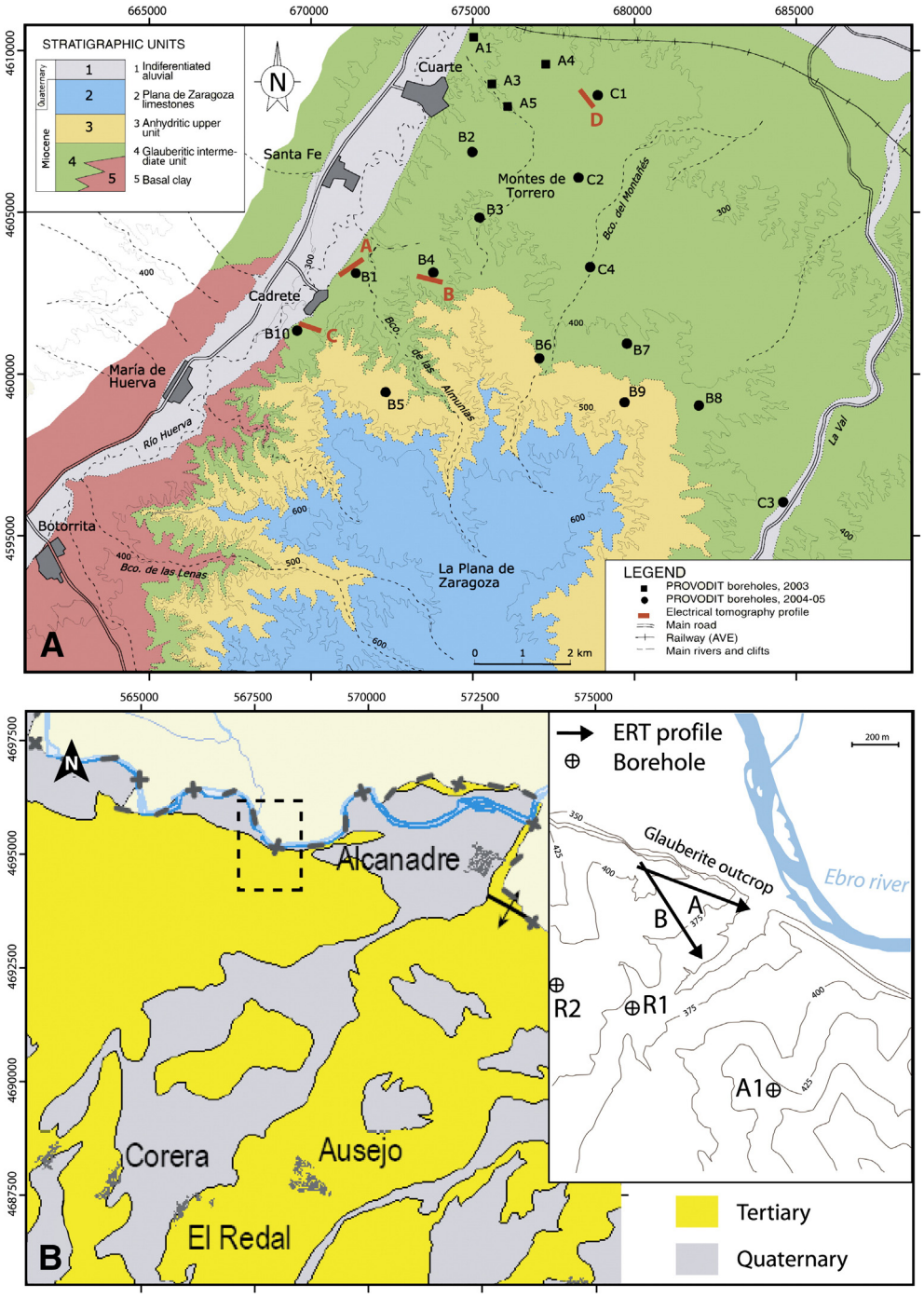

Fig. 2. A) Detailed geological mapping of the Montes de Torrero area (Zaragoza). A1 to C4 are the available boreholes, while A, B, C and D (in red) are the location of the performed ERT lines (modified form Salvany, 2009). B) Geological mapping of the Alcanadre area (La Rioja); the studied area is marked with a dashed line. The topographic information of this area is displayed at the right part of the image (modified from the geologic map of Comunidad Autónoma de La Rioja 2009). Location of both areas is shown in Fig. 1. The coordinates are given in Universal Transverse Mercator format, spindle 30. (For interpretation of the references to color in this figure legend, the reader is referred to the web version of this article.)

The glauberite deposit of Montes de Torrero is placed within the Zaragoza Gypsum Formation (close to the city of Zaragoza; Fig. 2A), developed during the Lower Miocene. In this area glauberite is never cropping out. However, layers of gypsum pseudomorphs after glauberite are common in many surface layers, together with sodium sulfate efflorescences and dissolution structures. This deposit was explored by a mining company during the 2000's through a large number of boreholes. Bellow the gypsiferous cover, glauberite is found as several tabular layers each one up to 20 m thick, developed within a unit mainly composed of secondary gypsum (at more superficial conditions) or anhydrite–halite (at depth). In these layers, glauberite is in part embedded in variable amounts of lutite matrix and partially cemented by halite (Salvany, 2009).

The glauberite deposit of Alcanadre is located within the upper levels of the Lerín Gypsum Formation, originated during the Lower Miocene (Salvany and Ortí, 1987; Fig. 2B), although earlier than the Montes de Torrero deposit. In this deposit, exceptionally, some glauberite and anhydrite layers crop out in a cliff excavated by the Ebro River, close to the village of Alcanadre. In this cliff some old artisanal mines are found; their galleries permit to enter several tens of meters into the formation. During the 1980's a drilling campaign was performed by a mining company, which provided valuable material for the study of the

mineralogy and petrology of this deposit (Salvany and Ortí, 1994). Bellow the gypsiferous cover, glauberite forms several lenticular shaped layers up to 1.5 m thick within a unit manly composed of secondary gypsum (in the outcropping cliff) or anhydrite (at depth). Glauberite is mainly present as large crystals of centimeters in size with variable amounts of lutite or carbonate (dolomite, magnesite) matrix. Subordinate polyhalite layers are also found. In the glauberite layers halite is totally absent.

3. Study method

The ERT is a geophysical technique whose objective is to determine the real electrical resistivity distribution in the subsurface. To this end, a DC current is injected in the terrain by two electrodes and the voltage passed through the terrain is measured in two different electrodes along a 2D profile. The investigation depth of this technique depends on the spacing between electrodes. After processing the measured data, a trapeze shaped image displaying the calculated real electrical resistivity distribution of the terrain is obtained. This image allows us to interpret the distribution of the different materials below the area where the survey took place. There are many different arrays in the electrical prospection, which display different lateral or vertical resolution and different depths (Ma et al., 1997; Furman et al., 2003; Szalai and Szarka, 2008; Szalai et al., 2009). In this study, Wenner alpha, Wenner–Schlumberger and Dipole–Dipole arrays have been tried. Wenner alpha was discarded after initial trials due to its smaller investigation depth. All sections were obtained using both Wenner–Schlumberger and Dipole–Dipole methods and in those performed on terrains with little topographic variations, both arrays showed similar results (Fig. 3A). Nevertheless, the sections obtained in areas with big surface elevation changes (e.g. nearby a cliff) showed Dipole–Dipole array to be very noisy and not corresponding with the previous knowledge of the area and in-situ observations (Fig. 3B). The RMS error is also lower for the inverted data sets measured with Wenner–Schlumberger

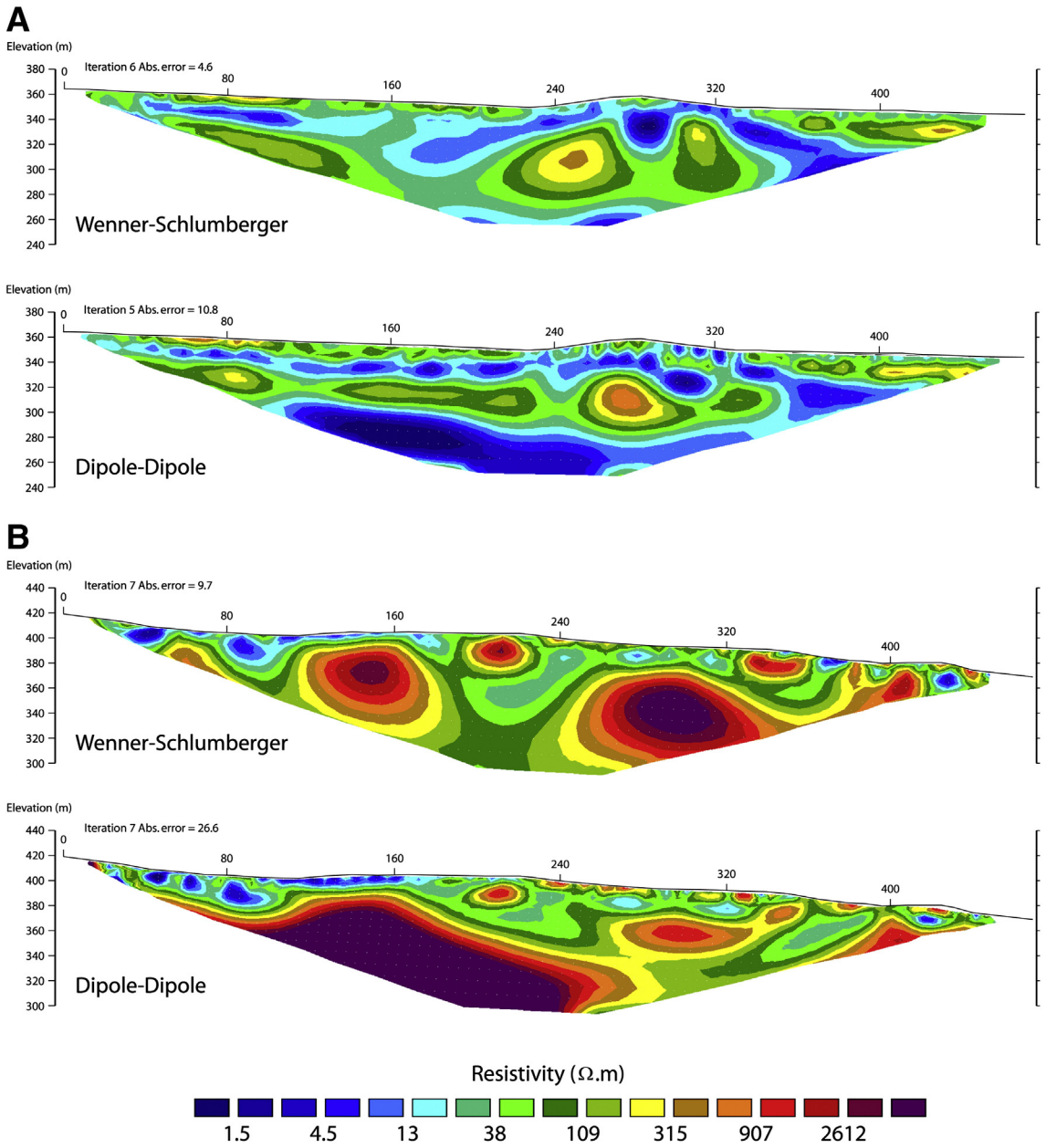

Fig. 3. Examples of inverted ERT sections measured using both Wenner–Schlumberger and Dipole–Dipole arrays in terrains with small (A) and large (B) topographic variations perpendicular to the resistivity lines. The presence of hills or cliffs as in B, generates large amount of noise in the deepest levels of the Dipole–Dipole sections.

(Fig. 3). For these reasons, only the results of Wenner–Schlumberger are displayed.

The resistivimeter used for the data acquisition was a Syscal Pro switch with 48 electrodes, 10 meter spacing between them and external power supply. The data was inverted with RES2DINV software, which uses the smoothness-constrained least-squares method (deGroot-Hedlin and Constable, 1990; Sasaki, 1992; Loke and Baker, 1996; Loke and Dahlin, 2002; Loke et al., 2003). The inverted resistivity data has been compared with information from boreholes. The studied sections in the Montes de Torrero area (Zaragoza) area were performed close to B1, B4, B10 and C1 boreholes (Fig. 2A). In Alcanadre area (La Rioja), the obtained resistivity sections have been compared with outcropping materials in the cliff and the different lithological levels showed on the available boreholes (Fig. 2B). All the performed resistivity sections have been performed upon the vadose zone; hence, the results do not represent terrains saturated with water.

Additionally to the ERT imaging, some sulfate samples were collected in the studied areas in order to evaluate the sulfate fraction of the deposits. The rock samples were powdered and afterwards 0.5 g were weighted and dissolved in 250 ml of distilled water. The solutions were shaken during 24 h. Thanks to the solubility of the sulfate minerals, these phases are dissolved in the distilled water so filtering the solution the residue left corresponds with the non-soluble phases. This remnant represents the fraction of matrix (carbonates, quartz and other accessory minerals). Thus, the matrix can be weighted and quantified.

The way in which structures in the sulfate rocks affect the resistivity distribution of the terrain has been studied by means of 3 model blocks (Fig. 4) elaborated with RES2DMOD software, which calculates the electrical apparent resistivity pseudosection for a user-defined 2D underground model (Loke, 2002). This program has been widely applied for simulating the acquisition of field data in a terrain with a known resistivity distribution (Cornacchiulo and Bagtzoglou, 2004; Maillet et al., 2005; Sumanovac and Dominkovic, 2007; Srinivasamoorthy et al., 2009). The models elaborated simulate one of the deposits studied in Montes de Torrero, corresponding to the section in the borehole B10, and one of the deposits studied in Alcanadre, representing the section parallel to the cliff. In these two deposit dissolution processes (Montes de Torrero), thickness and compositional variations (Alcanadre) occur (Fig. 5). The shallower part of the Alcanadre section model was made with the in-situ observations of the cliff as reference, but the deeper levels were interpreted from the borehole information and the original field ERT section. In the studied areas no cavities were identified but, as this type of structures may be also found in glauberitic deposits, an additional model has been made representing a cavity identified in a sulfate quarry located in the locality of Beuda (Girona, Spain). The original field ERT section is also displayed for comparison (this section was measured using similar settings to those described before).

The forward modeling of the theoretical model blocks was calculated for each case. The data was processed afterwards with the program RES2DINV. The array selected was Wenner–Schlumberger, following

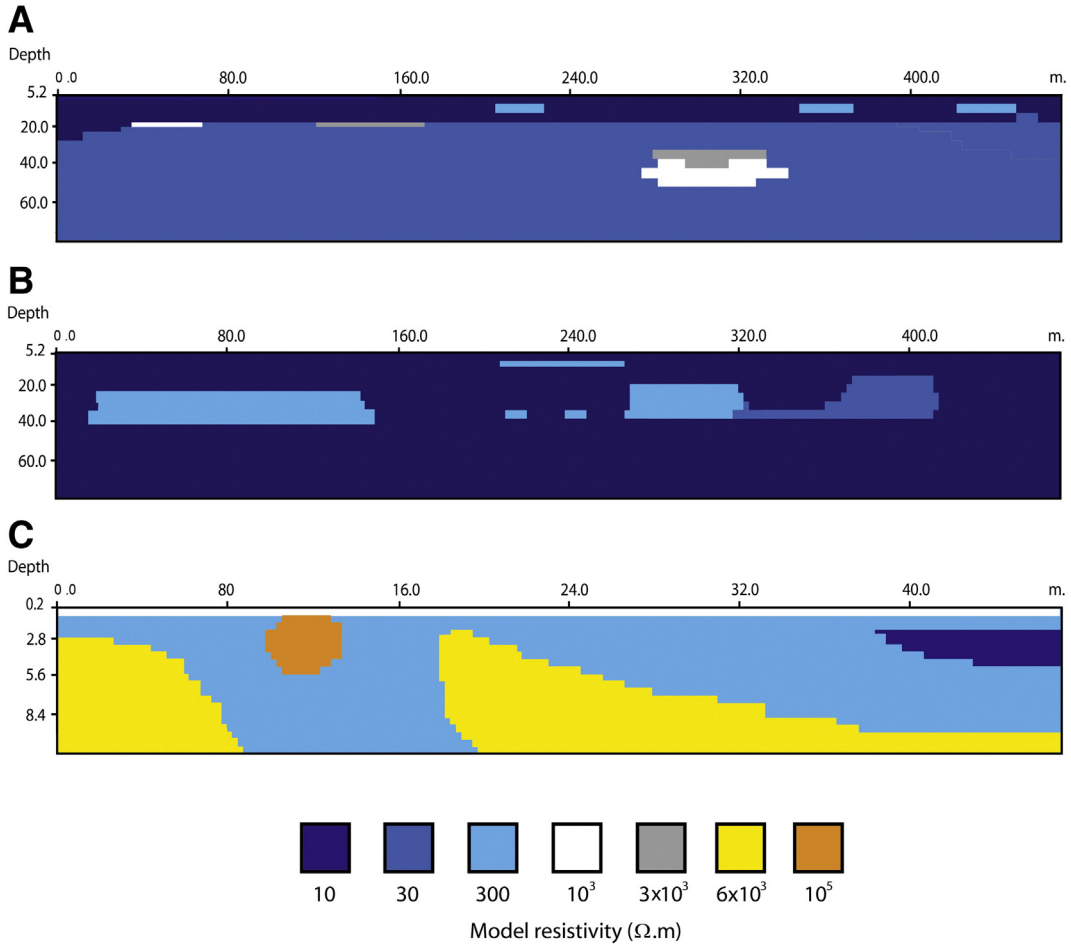

Fig. 4. Model-blocks representing typical structures in sulfate rocks. White color indicates pure gypsum; light blue, gypsum with high matrix fraction; dark blue, lutites; and orange, air-infilled cavities. A) Simple lateral compositional variation; B) complex lateral and vertical compositional variation; C) totally infilled karst cavities; and D) empty karst cavities in gypsum. (For interpretation of the references to color in this figure legend, the reader is referred to the web version of this article.)

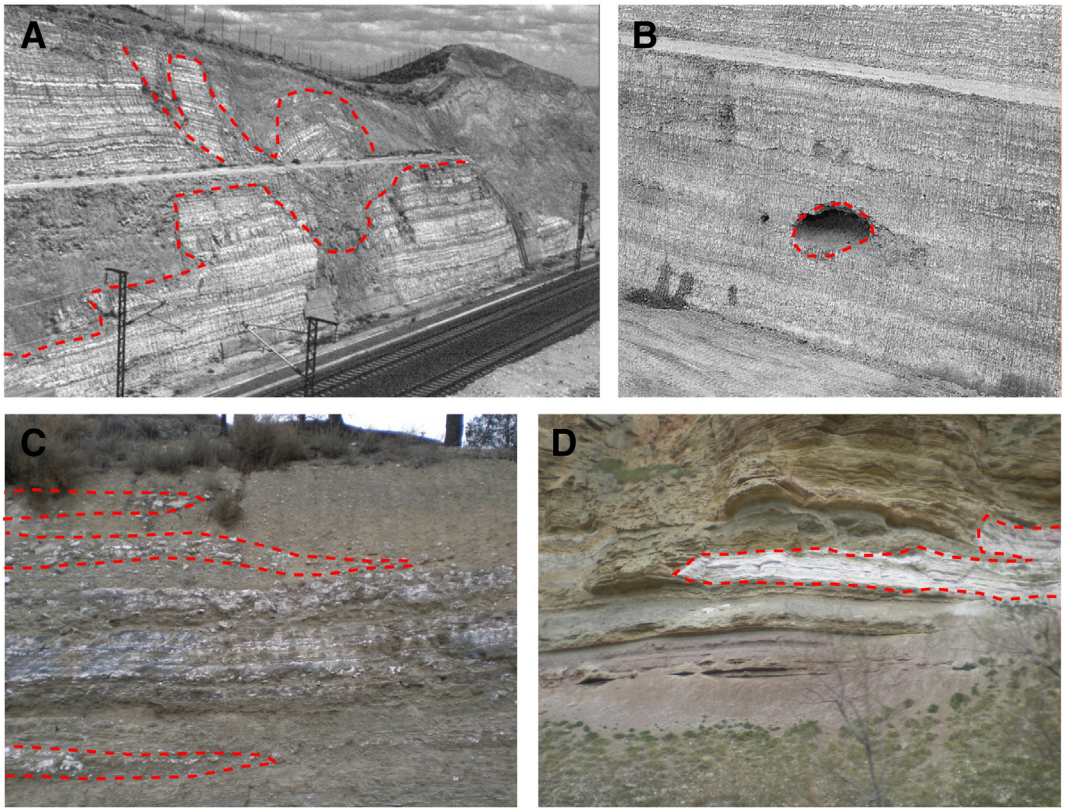

Fig. 5. Photographs of the most common structures in sulfate rocks. A) Gypsum karstification filled by lutites (modified from Guerrero et al., 2003); B) tunnel in a gypsum formation (modified from Guerrero et al., 2003); C) lateral thickness variations in gypsum layers; and D) pure glauberite layer disappearing laterally.

the case of the field examples. The selected electrode spacing varies in each case to be in accordance with the original section. All models have been elaborated to simulate deposits with a mixture of glauberite, and gypsum rocks with different compositions (10 to 10^3 Ω·m depending on the gypsum fraction and $>10^3$ Ω·m for anhydrite; Guinea et al., 2010a). The resistivity value selected for the cavities is the maximum which can be selected by the program RES2DMOD: 10^5 Ω·m (this value is higher than any geologic material).

4. Results

4.1. Montes de Torrero area (Zaragoza)

In Montes de Torrero area four ERT profiles have been carried out in accordance with the situation of boreholes B1, B4, B10 and C1 (Fig. 2A). The profiles have been performed with the boreholes situated on their center with the exception of B10, which is situated on the western side and topographically some few meters above the tomographic line.

The outcropping materials close to B1 borehole (Fig. 6A) show low sulfate contents (gypsum, anhydrite and/or glauberite in any combination) with a large quantity of matrix on them. The inverted electrical resistivity profile (Fig. 7A) shows a general low resistivity trend with values below 50 Ω·m on it. The log of the borehole has a great quantity of matrix at any depth; similarly to outcropping rocks. Some sulfate layers show lower matrix contents, but their composition is always below 50% in the different sulfate mineral fraction (gypsum, anhydrite and/or glauberite; Fig. 8A). At a depth of 60 m there is the purest layer of glauberite of the whole borehole and the fraction of the rock in glauberite mineral is above 50%. This is not shown in the resistivity section due to both the low sensitivity of the method at this depth and the little thickness of the layer.

In the areas of boreholes B4 and B10 the composition of the evaporitic layers is also dominated by matrix (Fig. 6B) and there are evidences of dissolution processes (Fig. 6C). In some locations, glauberite appears in surface as pseudomorphs of gypsum (Fig. 6D). The inverted profile of the B4 borehole (Fig. 7B) shows low resistivity values due to the low sulfate fraction of the deposit. Approximately at a depth between 20 and 60 m (depending on the position) the resistivity increases defining a laterally discontinuous structure. This structure is probably associated to changes in sulfate fraction of the rocks (Fig. 8B). B4 borehole has lesser matrix quantity below a depth of 40 m, in accordance with the structure displayed in the profile. The lateral compositional variation of this level is probably bounded to depositional primary processes. The resistivity value of this structure is up to 300 Ω·m. In the bottom part of the image the resistivity decreases, suggesting a sulfate fraction similar to the shallowest layers. This is also shown in the B4 borehole. The sharpest lateral resistivity changes (especially in the NW part of the profile), may be related to dissolution processes and posterior infilling.

The resistivity section of B10 borehole was performed in dry ephemeral creek streambed. The resistivity section (Fig. 7C) is similar to that of profile B. There are three layers of low resistivity and the one in the middle is more resistive and discontinuous. In this case, the discontinuity of the most pure layer has sharp-vertical bounds instead of progressive and undefined as in profile B; these structures are related to dissolution processes and infilling affecting the area related to the creek (Fig. 8C). The depth of the layer with transitional resistivity value fits with the depth of glauberite levels observed in B10 borehole. The interpretation of this section has been made in accordance with the theoretical model representing the same ERT line (Fig. 4B).

The area surrounding C1 borehole is covered by quaternary soil. This area is located several kilometers from the other three studied boreholes (Fig. 2A). The inverted resistivity section (Fig. 7D) shows a

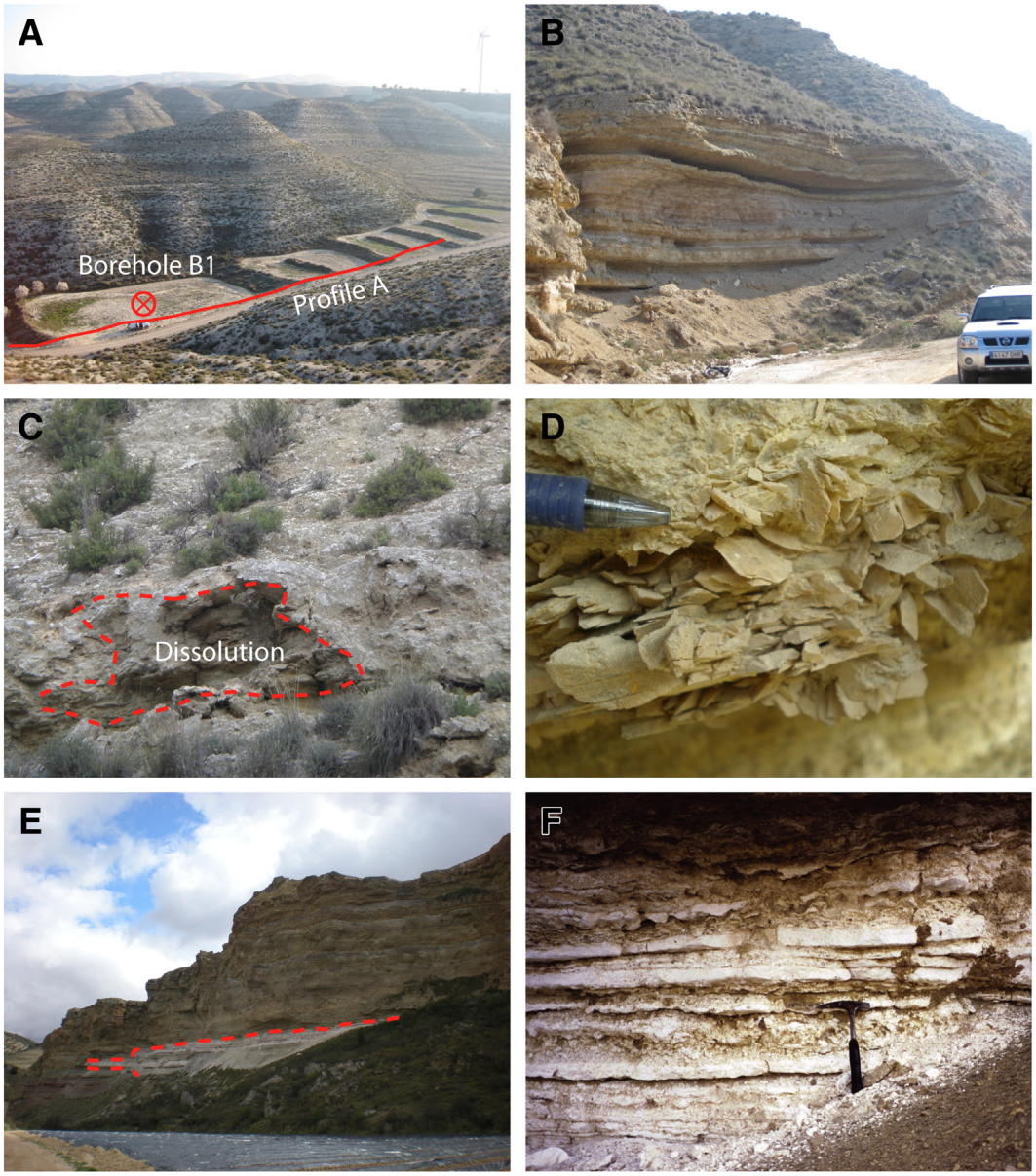

Fig. 6. Photographs of the outcropping evaporitical units in the Montes de Torrero (Zaragoza; A, B, C and D) and Alcanadre (La Rioja; E and F) areas. A) General view of Montes de Torrero region in the area of B1 borehole; B) view of layered-nodular gypsum–lutites sequence in the profile C; C) superficial dissolution processes (red dashed line); D) detail of outcropping glauberite pseudomorphs (hydrated to secondary gypsum) in the profile C; E) general view of the evaporitical materials conforming the cliff in Alcanadre area (La Rioja); the glauberite layer is marked with a red dashed line; and F) detailed view of the glauberite deposit in which the layering can be appreciated. (For interpretation of the references to color in this figure legend, the reader is referred to the web version of this article.)

complex distribution of the terrain with both lateral and vertical discontinuities. In comparison with the previous sections, larger values of the resistivity are observed. In the center of the profile at a depth of approximately 20 m, there is a local increasing on the resistivity of the deposit. The resistivity reaches values of rocks with low matrix fraction. In C1 borehole it is observed a quite pure sequence with some relatively thin clayey levels interlayered. The fraction in matrix increases at the bottom of the profile where there is a change from gypsum and glauberitic layers to anhydritic layers, as it is observed in the log of C1 borehole (Fig. 8D).

4.2. Alcanadre area (La Rioja)

In the Alcanadre area a cliff excavated through evaporite deposit by the Ebro River has been studied. Nearby boreholes R1, R2 and A1 were also available (Fig. 2B). In those boreholes, glauberite-rich layers were found at different depths. In all of them, the top of the glauberitic sequence has been identified at a topographical elevation of approximately 330 m (Fig. 9).

Regarding the rocks on the cliff, there is an unusual outcropping pure layer of glauberite. This layer is white in appearance due to efflorescence precipitation (sodium sulfate; Fig. 6F) and laterally wedges eastward (Fig. 6E). Towards the west there are fallen materials covering the outcrop so its lateral continuity is unknown in that direction. Samples have been taken from the pure glauberite layer in order to measure the quantity of insoluble matrix, and above 95% in sulfate minerals have been calculated.

The geoelectrical survey has been performed in the upper part of the cliff (Fig. 2B). Two ERT profiles have been performed with the aim of identifying the pure glauberite deposit observed in the cliff and define

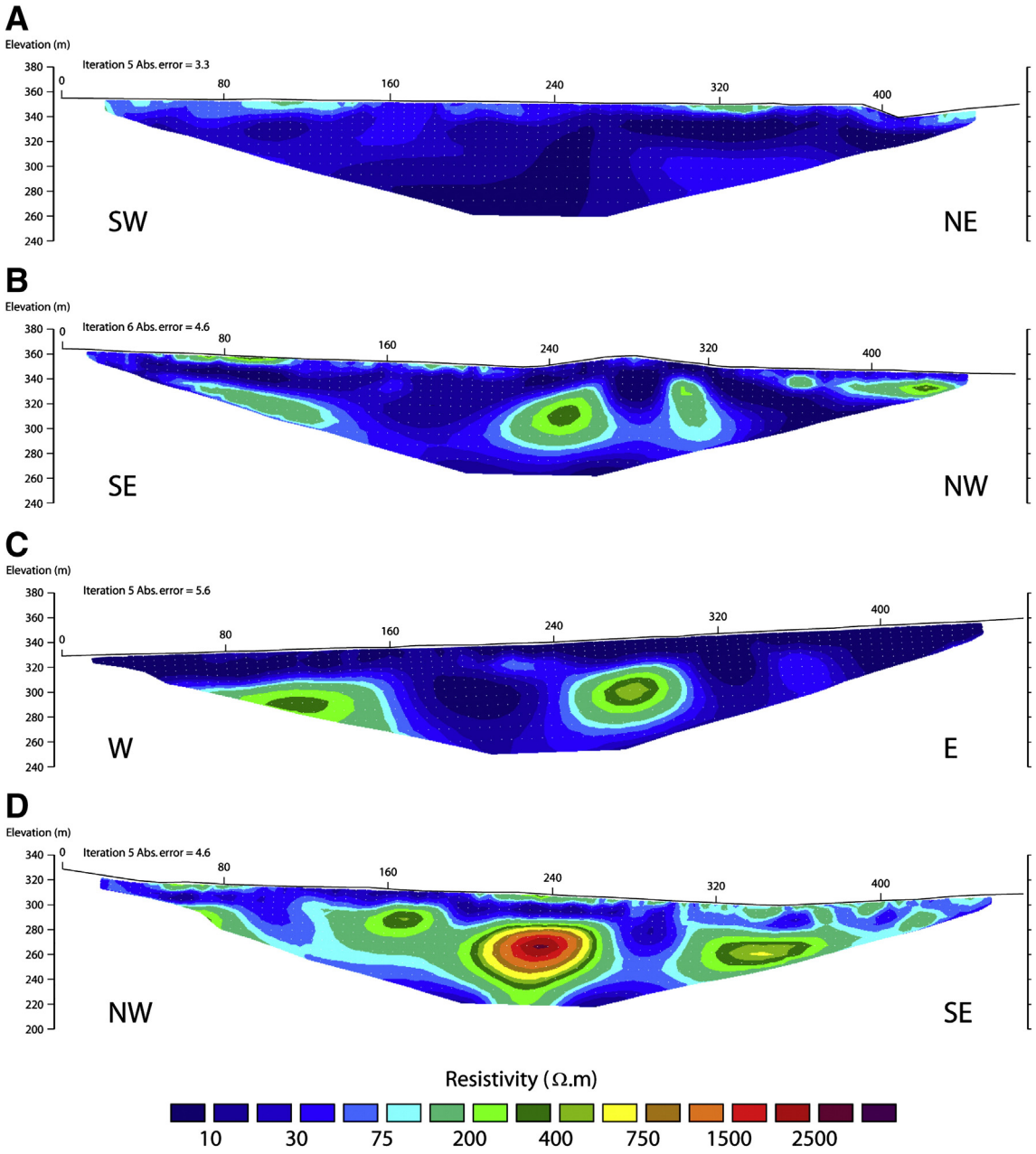

Fig. 7. Inverted resistivity images of Montes de Torrero area (Zaragoza). The location of the profiles is shown in Fig. 2A.

the electrical resistivity value of glauberite in a deposit with high glauberite fraction. The profile A has been performed parallel to the cliff and the profile B obliquely. In the cliff, the secondary gypsum cover is approximately 20 m thick, but in the area in which the profiles have been carried out, there is a topographic depression. Therefore, the depth of the layer from the surface is approximately 12 m. In the cliff is observed that the layers below the glauberite layer are made of matrix-rich gypsum; similarly to the upper part.

In the inverted section of profile A (Fig. 10A), a heterogeneous distribution of the resistivity is shown. The section observed in the cliff, corresponds with the horizontal stretch between 100 and 200 m. The shallowest low resistivity layer is related to the matrix-rich gypsum rocks. Below these layers, the resistivity increases, achieving values up to 2.5×10^3 Ω·m in rectangular-shaped bodies. In the part of the profile coinciding with the position of the cliff, there is one of those resistive bodies at the depth in which the pure glauberite layer is observed, displaying the shape of a lens. The resistive body of the SE probably corresponds with another similar deposit. The lack of lateral continuity of the glauberite layer has been observed in the cliff (Fig. 6E) as well as in the resistivity section. At the bottom of the profile the resistivity decreases because of the matrix fraction increasing in the composition of the rocks. The profile B (Fig. 10B) displays a similar resistivity distribution of the terrain. In this case the glauberite layer observed in the cliff is also showed as a resistive body (up to 3×10^3 Ω·m) in the NW part of the profile. This section of the lens is located a few meters south of the one observed in Profile A. In the SW part of the profile (which is the furthest one from Profile A) there is no resistive body present.

4.3. Theoretical models

The inverted resistivity sections based in the models representing field-sections of both Alcanadre (Fig. 11A) and Montes de Torrero (Fig. 11B) show a reasonable resemblance to the original sections (Figs. 7C and 10A). The implications are discussed in Section 5.3.

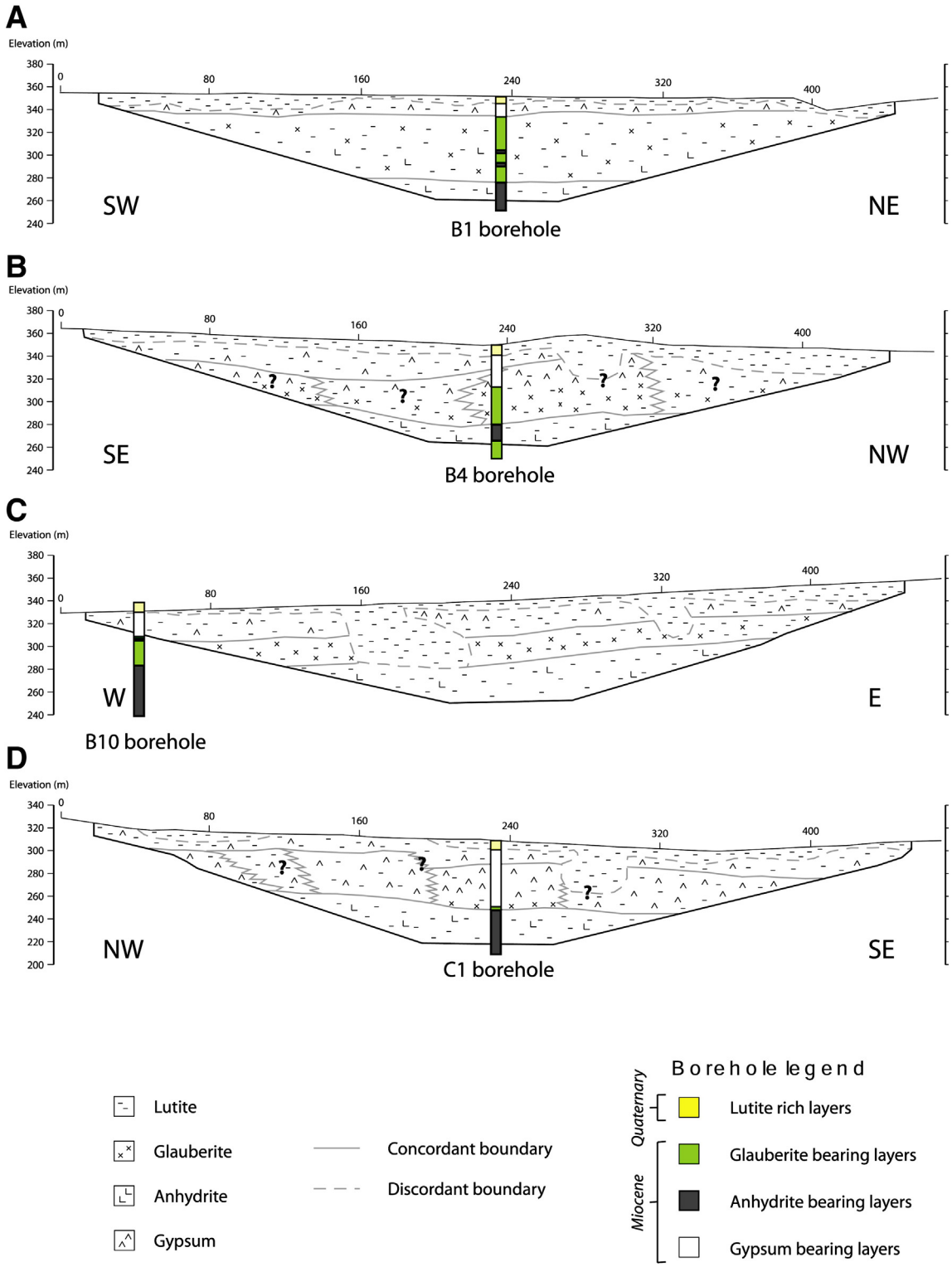

Fig. 8. Geological interpretation of the ERT profiles shown in Fig. 7. The relative proportion of sulfate and matrix contents is indicated by the amount of the legend signs. The question marks indicate areas in which the interpretation is uncertain. There is a superimposed synthetic representation of the boreholes B1, B4, B10 and C1 located in their relative position on the profiles. The situation of the profiles is showed in Fig. 2A.

The inverted field ERT section obtained in the sulfate Quarry of Beuda displays a very heterogeneous electrical resistivity distribution. Highly resistive anomalies (>5000 Ω·m) are found in several positions along the section (Fig. 11C). However, in the left part of the section an unusually high resistivity anomaly (>2×10^5 Ω·m) is displayed. The model made based in this profile also shows similar inversion results (Fig. 11D).

5. Discussion

5.1. Electrical resistivity of glauberite rocks

As it has been previously mentioned, no references regarding the electrical properties of glauberite rocks have been reported. In the glauberite deposit of Alcanadre area (La Rioja), a mean resistivity of

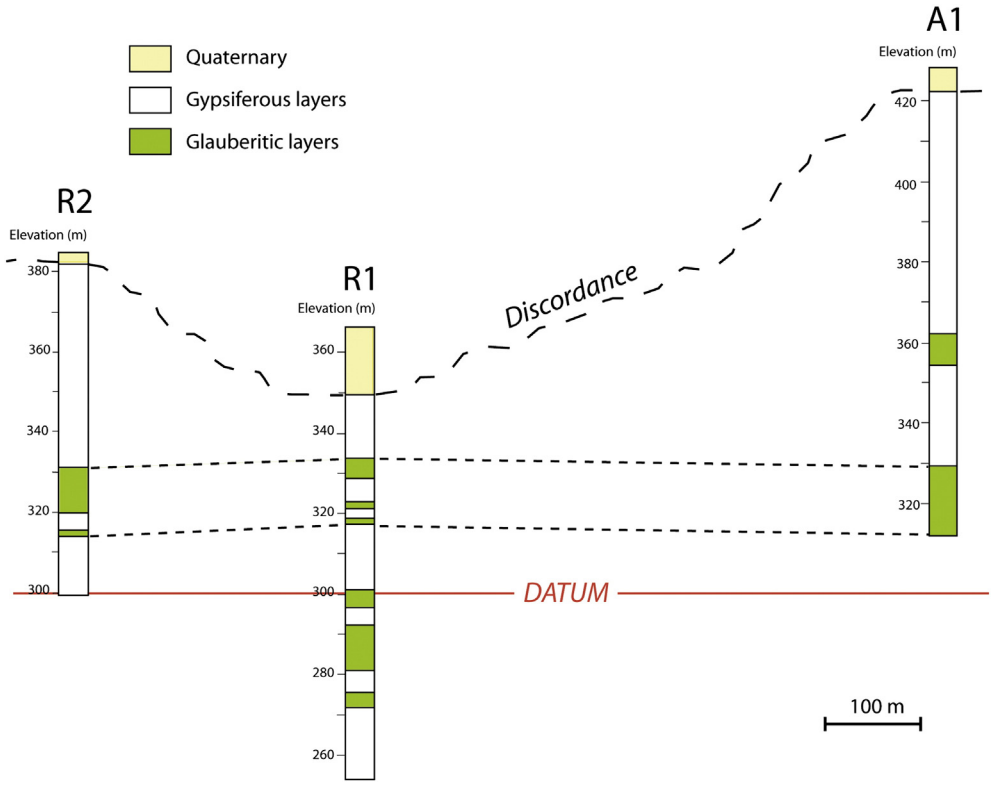

Fig. 9. Synthetic representation of the boreholes A1, R1 and R2 in the Alcanadre area (La Rioja). The possible correlation between layers is marked with dashed lines; this correlation of the logs has been made considering the topographic elevation. The location of the boreholes is displayed in Fig. 2B.

approximately 3×10^3 Ω·m has been calculated (Fig. 10). The studied glauberite level is sulfate-rich (95%), but the glauberite is probably mixed with certain amount of gypsum; hence this value is only a reference. In any case, pure glauberite has shown to be more resistive than gypsum (10^3 Ω·m) and probably less than anhydrite (10^4 Ω·m). In most cases, it is not possible to differentiate between bodies of 10^3 and 3×10^3 Ω·m with ERT unless they are close to the surface (where the method is more sensitive), because they are in a similar range of values.

Glauberite rocks bear different sulfate phases besides glauberite crystals and the matrix component. It can be considered that the sulfate

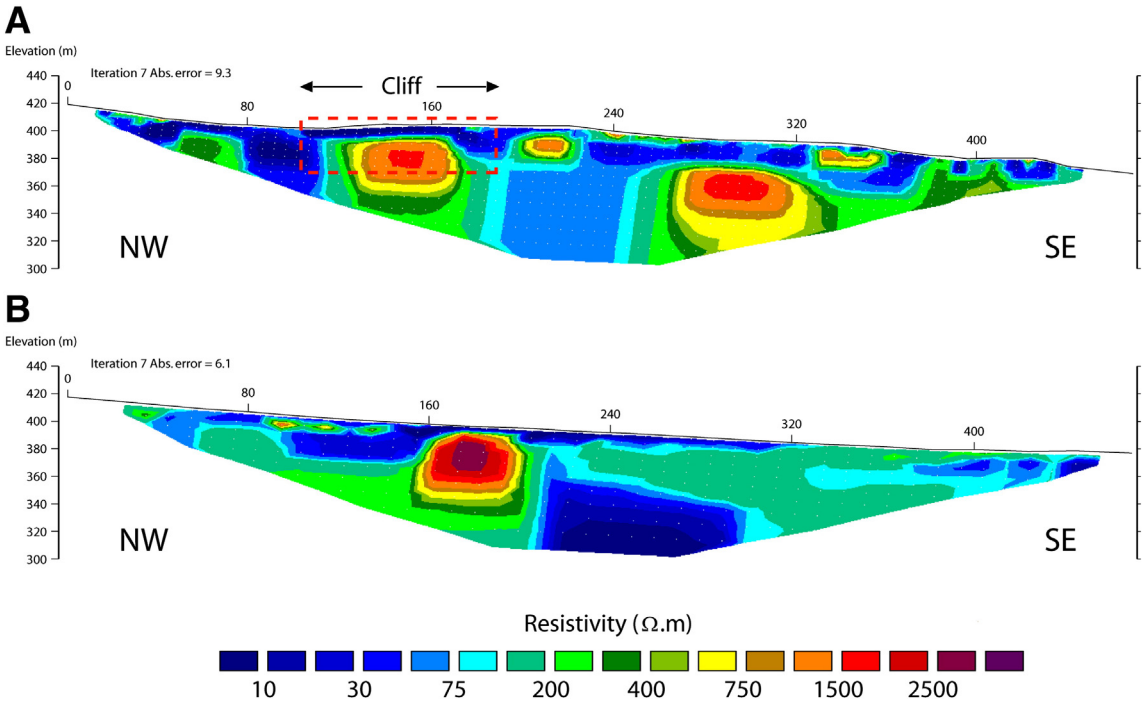

Fig. 10. Inverted resistivity images of Alcanadre area (La Rioja). The position of the cliff (parallel to the profile) is marked with a red dashed square in profile A. The situation of the profiles is shown in Fig. 2B. (For interpretation of the references to color in this figure legend, the reader is referred to the web version of this article.)

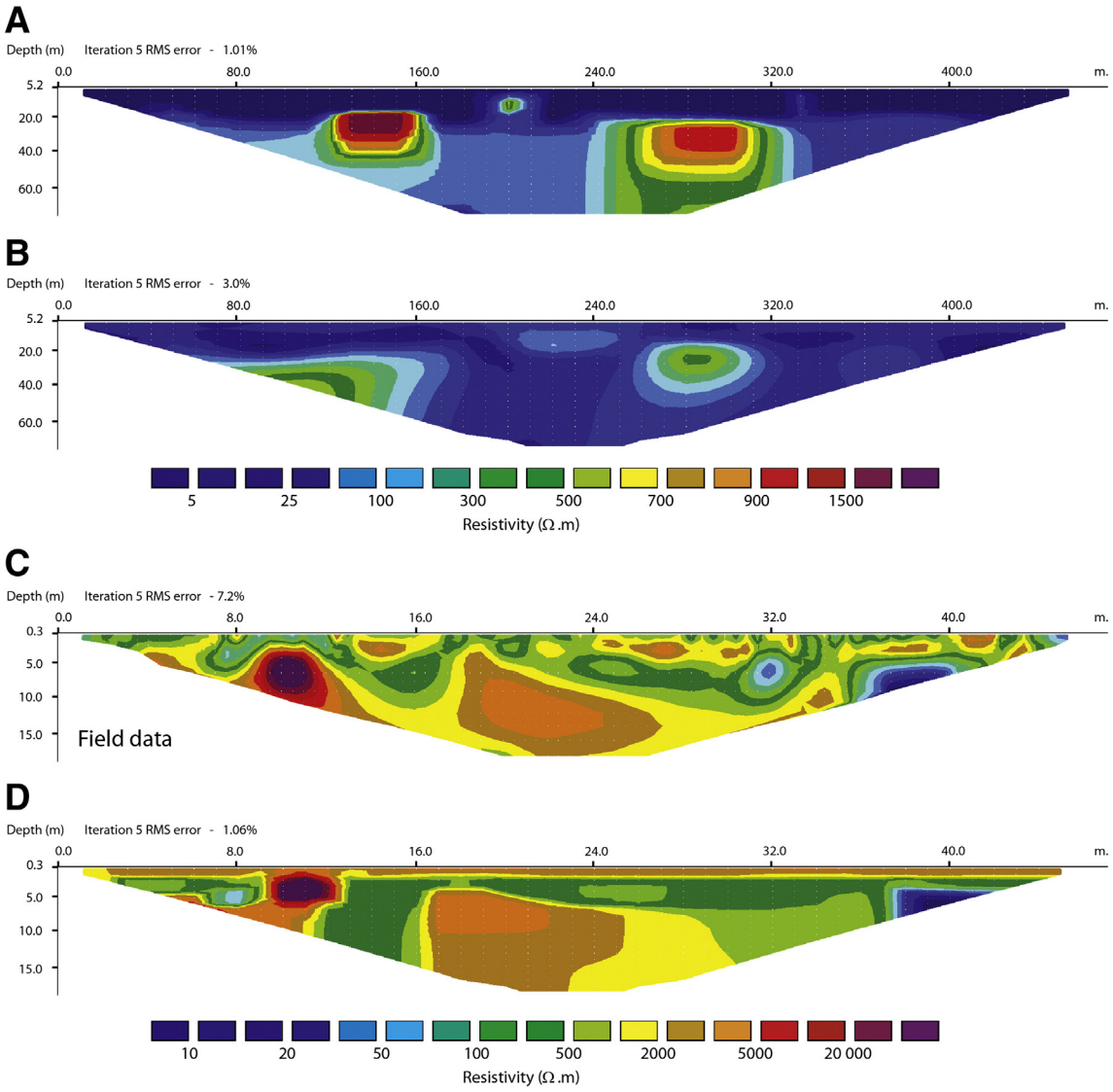

Fig. 11. Inverted resistivity profiles of the direct models obtained from Fig. 4. The resistivity changes in the original models are marked with dashed lines.

component is made of a combination of gypsum, anhydrite and glauberite, although other evaporitic minerals as chlorides may be present. Guinea et al. (2012) defined three resistivity domains of the calcium sulfate rocks depending on their composition (gypsum, anhydrite and matrix). These domains are conditioned by the quantity of matrix present in the rock. When the matrix represents 45% or more of the composition of the bulk rock (or ≤55% of sulfate content), the matrix is connected at long range (percolating matrix) and most of the electrical current spreads through it because is much more conductive than the sulfate phases. When the matrix fraction is 30% or below (or ≥70% of sulfate content), the electrical current finds no connected pathways through it and then runs through the sulfate phases, rapidly increasing the resistivity of the bulk rock. Between the matrix and the sulfate domains there is a transitional zone.

In order to predict the bulk conductivity of a porous medium, different mixing models can be found in the literature (Warren and Price, 1961; Shankland and Waff, 1977; Somerton, 1992; Guéguen and Palciauskas, 1994; Glover et al., 2000). The primary porosity in sulfate rocks is negligible; therefore, the effective conductivity of the bulk rock depends on the fraction (γ) and the electrical resistivity value (ρ) of each component and on the connectivity and geometrical distribution of the matrix (which has the role of a conducting fluid in a saturated porous medium). The Hashin–Shtrikman (HS) mixing model (Hashin and Shtrikman, 1963) can be used as an approximation to the resistivity trend of sulfate rocks (Guinea et al., 2012). The matrix domain shows a similar trend to the one of lower HS lower bound (HS^-), while the sulfate domain can be described with the HS upper bound (HS^+). The transitional zone does not fit to the trends showed by the HS bounds. The percolation phenomena described in the cases of calcium sulfate rocks can be also applied for the glauberite rocks. It is possible to calculate the HS bounds for a 4-phase system (glauberite, gypsum, anhydrite and matrix) from the general formula given by Berriman (1995) for n-phases, but this system is much complex than a case with only three phases and because of that usually simplifications are used (Torquato, 2002). Furthermore, the representation of this 4-phase system is tetrahedral, which makes it very complicated to be used. In any case, for rocks with 45% or more in matrix fraction (within the matrix dominium), a binary system sulfate–matrix can be considered because, as previously stated, the electrical current runs through the matrix avoiding the sulfate phases. Two-phase system HS bounds (Table 1a and b) of glauberite–matrix, anhydrite–matrix and gypsum–matrix have been calculated to evidence that there are no significant differences between their HS^- bounds (Fig. 12). The resistivity value selected for pure glauberite was $3 \times 10^3\ \Omega \cdot m$, which is the higher resistivity calculated from field data (in Alcanadre area). This value is an approximation, but its exactitude is not important as it will be discussed later. For

Table 1
Summary of Hashin–Shtrikman equations for the case of two (A and B; Hashin and Shtrikman, 1963) and three (C and D; Berriman, 1995) phase systems.

Name	Conducting phases	Equation
a. Hashin–Shtrikman upper bound	2	$\sigma_{eff+} = \sigma_2\left(1\frac{3(1-\chi_2)(\sigma_2-\sigma_1)}{3\sigma_2-\chi_2(\sigma_2-\sigma_1)}\right)$
b. Hashin–Shtrikman lower bound	2	$\sigma_{eff-} = \sigma_1\left(1+\frac{3\chi_2(\sigma_2-\sigma_1)}{3\sigma_1+(1-\chi_2)(\sigma_2-\sigma_1)}\right)$
c. Hashin–Shtrikman upper bound	3	$\sigma_{eff+} = \frac{1}{\left(\frac{\chi_1}{\sigma_1+\sigma_2}\right)+\left(\frac{\chi_2}{3\sigma_2}\right)+\left(\frac{\chi_3}{\sigma_3+2\sigma_2}\right)}-\sigma_2$
d. Hashin–Shtrikman lower bound	3	$\sigma_{eff-} = \frac{1}{\left(\frac{\chi_1}{\sigma_1+2\sigma_3}\right)+\left(\frac{\chi_2}{\sigma_2+2\sigma_3}\right)+\left(\frac{\chi_3}{3\sigma_3}\right)}-2\sigma_3$

the gypsum and anhydrite phases, 10^3 and 10^4 Ω·m respectively were selected, according to Guinea et al. (2010b, 2012). Rocks with composition in the transitional zone (sulfate fraction between 55 and 70%), will show resistivity values between the HS^- and HS^+.

In the case of the glauberite rocks with a composition of 70% or above in sulfate fraction (in the sulfate dominium), the matrix is non-percolating and therefore, the resistivity of the bulk rock is conditioned by the composition of the sulfate phases, following the trend of the 4-phase HS^+ for that composition range. As a simplification, the HS^+ of 3-phase system (glauberite, gypsum an anhydrite; Table 1c) have been calculated in 4 different diagrams (Fig. 13), considering a constant fraction of matrix (30, 20, 10 and 0% respectively). Unlike the matrix-percolating compositions, in the sulfate domain the quantity of each sulfate component has a direct influence in the resistivity of the rock. The trend of the resistivity is similar for any matrix composition (considering 30% or below), being the anhydrite the most influent phase; but increasing the resistivity gradient when the matrix fraction is lower.

The resistivity ranges observed in the diagrams overlap for a lot of different compositions. Hence, it is not possible to interpret the composition from the resistivity; additional information must be obtained (as boreholes) to identify the different sulfate minerals on the deposit. The diagrams for compositions in the sulfate dominium do not provide significant information and therefore, it is not possible to elaborate a classification from them, but they show the evolution of the complexity of the bulk rock resistivity as more phases are added to the system.

In any case, in most of glauberite deposits the glauberite crystals will be mixed with an important amount of matrix (in the matrix-percolating domain) and, thus, they will display the resistivity range

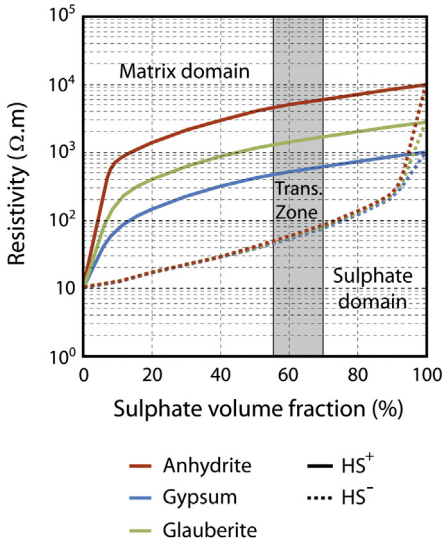

Fig. 12. Hashin–Shtrikman upper (HS^+) and lower (HS^-) bounds for two phase systems (sulfate and matrix). Upper bounds are displayed with continuous lines while lower bounds are represented with dotted lines. Sulfate rocks in the matrix domain will show the trend of lower bounds, which overlap.

of the HS^- of any sulfate–matrix system, which corresponds with the electrical response of the matrix and it is non-dependent on the composition of the sulfates. Therefore, the resistivity range of the glauberite crystals has no influence on the resistivity of the bulk rock. It does not matter if glauberite has a resistivity of 3×10^3 Ω·m or higher because the HS^- bound does not change. This means that the range of resistivity values of the glauberite rocks oscillates approximately between 10 and 100 Ω·m for regular deposits (matrix-rich), and higher values will be related to the presence of gypsum, anhydrite and/or other evaporitic minerals (sulfate-rich rocks).

5.2. Field data

The evaporitic sequence in Montes de Torrero (Zaragoza) has high matrix content. Locally, the sulfate fraction may be higher but without lateral continuity; this would be the case of the profile associated with the C1 borehole (Fig. 7D). As most of the studied materials (profiles of boreholes B1, B4 and B10; Fig. 7A, B and C) are in the matrix and transitional domains (according to the geoelectrical classification proposed in the Fig. 12), there is no way of differentiating glauberite from gypsum or anhydrite only from the resistivity data. Nonetheless, electrical imaging is useful for observing the distribution of the terrain and to identify the areas with larger sulfate contents, although parametric boreholes are necessary for a suitable interpretation of the sections (as in Fig. 8). Many primary and secondary complex structures are shown in the resistivity sections and they are difficult to be interpreted. The evaporitic sequence of Montes de Torrero represents a typical glauberite deposit.

As in the sections of Montes de Torrero area, great complexity of the resistivity distribution of the terrain is displayed in Alcanadre area (La Rioja). The sulfate fraction of the purest glauberite lens sampled in the cliff is rarely high. The studied glauberite body is detected in both inverted profiles, but its thickness is exaggerated (Fig. 10). This is because below the resistive layers, the Wenner–Schlumberger array tends to create resistive shadows due to the decreasing sensitivity of the method. In the profile parallel to the cliff (Fig. 10A), another possible glauberite lens (highly resistive body) is identified in the SE part of the section. The rest of the materials show matrix-domain resistivities; these matrix-rich materials are correlated with the lithologies observed in the cliff (Fig. 6E). The second lens is not showed in the profile performed obliquely to the cliff (Fig. 10B). R1, R2 and A1 boreholes (Fig. 9) evidence the presence of several discontinuous glauberite levels. It is probable that there are some other glauberite layers at different depths which are not identified with the electrical imaging due to their low content in sulfate crystals.

5.3. Theoretical models

The inverted section of the model simulating the deposit of Alcanadre in the section parallel to the cliff is an example of deposition-originated compositional changes in a glauberitic deposit (Fig. 11A). The higher resistivity anomalies are generated by local increase of sulfate fraction. The ERT inverted section obtained from the model representing the B10 borehole section in Montes de Torrero displays a dissolution structure filled with lutites. These structures were known from field observation,

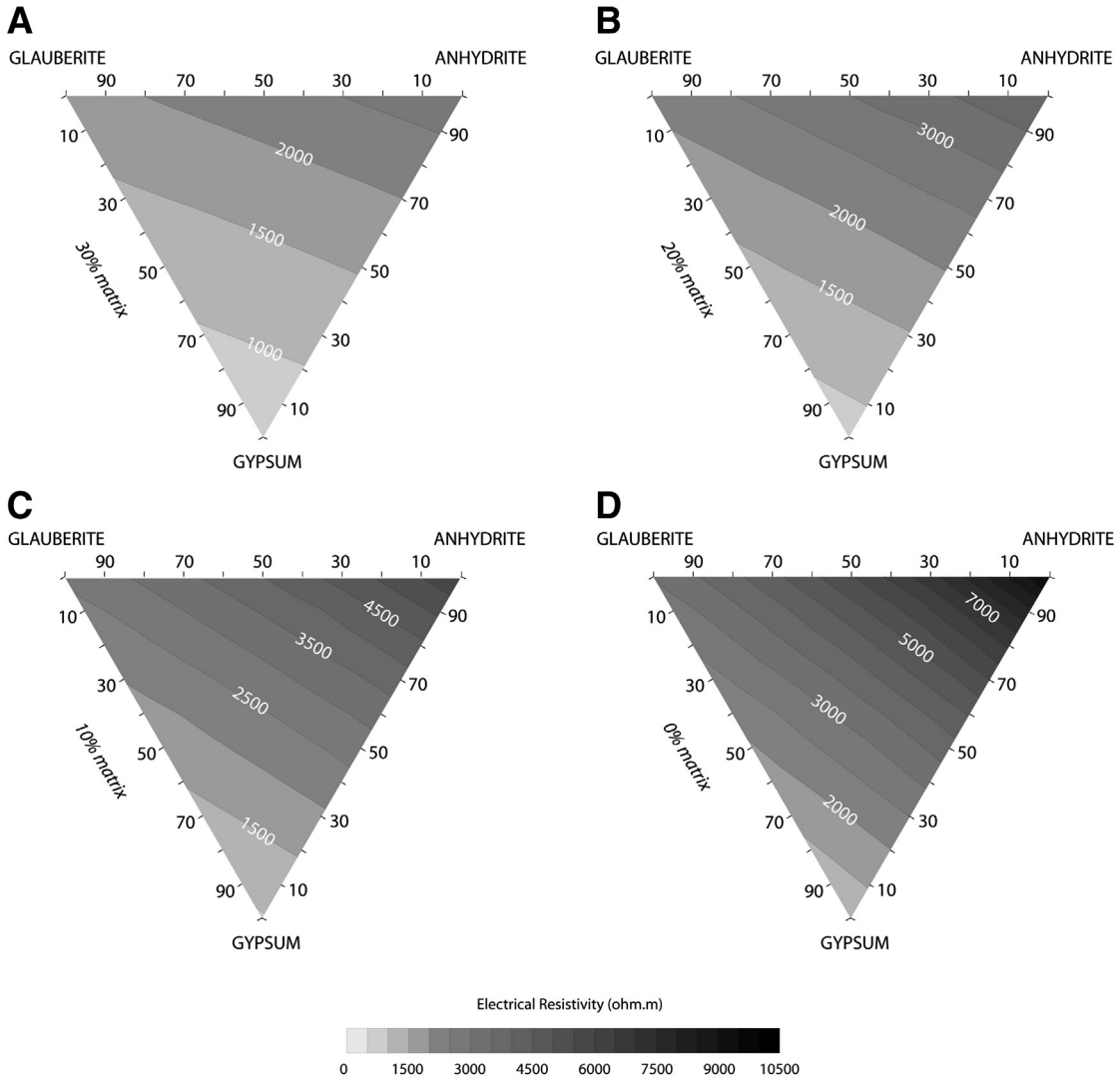

Fig. 13. Hashin–Shtrikman upper bounds for glauberite rocks with sulfate fractions of 70% (A), 80% (B), 90% (C) and 100% (D) in the case of the 4-phase glauberite–anhydrite–gypsum–matrix system. The representation is displayed as 3-phase systems with different constant quantities of matrix (30%, 20%, 10% and 0%).

but they also have a slightly different signature in the resistivity distribution compared to compositional changes (Fig. 11B). If little variation in the composition of the sulfate level exists, the resistivity in both sides of the dissolution structure should remain similar as it happens in this case.

The heterogeneous distribution of the resistivity in the Quarry of Beuda section (Fig. 11C) corresponds to an equally heterogeneous composition. The highly resistive anomalies (>5000 Ω·m) correspond in most cases to anhydrite bodies, but the anomaly with resistivity >2 × 10^5 Ω·m is generated by a cavity that has also considered in the model section (Fig. 11D). It has to be noted that this type of structures would not be possible to detect in the areas of the ERT sections with low sensitivity (e.g. in the deepest part of the section) due to the inaccuracy in the resistivity calculation.

Even though the models described here are a good approximation to the typical structures present in glauberite deposits, it has to be considered that they only are a rough approximation of the real cases, where the level of compositional complexity is very high.

6. Conclusions

Electrical resistivity lines are useful for the prospection of glauberite rocks, but these surveys should be supported by parametric drilling works. In any case, the number of required boreholes for the characterization of the deposit decreases considerably if this technique is considered. Additionally, geoelectrical prospecting should be supported by an additional petrological study of the deposits in order to properly interpret the resistivity profiles. The knowledge about the quantity of matrix within the rock is essential because his presence decreases the electrical resistivity values hiding the real values of the sulfate phases.

Pure glauberite rocks have displayed a calculated electrical resistivity value up to 3 × 10^3 Ω·m in Alcanadre (La Rioja); this is the first reference to the electrical resistivity of glauberite rocks proposed in the literature. Taking this value as a reference, the Hashin–Shtrikman bounds can be calculated for a 4-phase system (gypsum, anhydrite, glauberite and lutite matrix), but due to its complexity it has been simplified to 2 and 3-phase diagrams. In the case of glauberite rocks with a matrix fraction of 45% or above, the resistivity is bounded to the lower HS boundary. Hence, it can be considered as a 2-phase system (undifferentiated sulfate and matrix) because the matrix is the conductive dominating phase and the resistivity values are controlled by its presence. The electrical resistivity range in the case of sulfate-rich rocks with different compositional combinations (gypsum, glauberite, anhydrite) overlap and, therefore, it is not possible to establish a classification. In any case, most of the glauberite deposits are matrix-dominant and hence, will show values of matrix-percolating rocks (10–100 Ω·m); as in the case of Montes de Torrero (Zaragoza).

Even with the necessity of borehole information to carry out a suitable interpretation, ERT permits the detection of some structures, such as depositional systems or karst infillings. Lateral compositional changes and dissolution features are the most common structures which are found in sulfate deposits.

Acknowledgments

The present work is a part of a PhD thesis supported by the "Programa General d'Intensificació de la Recerca" (Generalitat de Catalunya-UB) and the Spanish Government Projects CGL2009-11096, CGL2009-07025, CGL2010-18260 and CGL2009-07604. We want to acknowledge the support and facilities of Dr. Albert Casas (Universitat de Barcelona), Landon Halloran (University of New South Wales) and Minera de Santa Marta SA, as well as the constructive comments of the reviewers.

References

Berriman, J.G., 1995. Mixture theories for rock properties. In: Ares, T.J. (Ed.), Rock Physics and Phase Relations: a Handbook of Physical Constants. American Geophysical Union, Washington, p. 236.
Cornacchiulo, D., Bagtzoglou, A.C., 2004. Geostatistical reconstruction of gaps in near-surface electrical resistivity data. Vadose Zone J. 3, 1215–1229.
deGroot-Hedlin, C., Constable, S., 1990. Occam's inversion to generate smooth, two-dimensional models from magnetotelluric data. Geophysics 55, 1613–1624.
Furman, A., Ferré, P.A., Warrik, A.W., 2003. A sensitivity analysis of electrical resistivity tomography array types using analytical element modeling. Vadose Zone J. 2, 416–423.
Garret, D.E., 2001. Sodium Sulphate: Handbook of Deposits, Processing, Properties and Use. Academic press, p. 384 (eds.).
Glover, P.W.J., Hole, M.J., Pous, J., 2000. A modified Archie's law for two conducting phases. Earth Planet. Sci. Lett. 180, 369–383.
Guéguen, Y., Palciauskas, V., 1994. Introduction to the Physics of Rocks. Princenton University Press, p. 294 (eds.).
Guerrero, J., Gutierrez, F., Lucha, P., 2003. Paleosubsidence and active subsidence due to evaporite dissolution in the Zaragoza area (Huerva River valley, NE Spain): processes, spatial distribution and protection measures for transport routes. Eng. Geol. 72, 309–329.
Guinea, A., 2011. Geoelectrical Characterization of Sulphate Rocks. University of Barcelona, p. 264 (PhD thesis).
Guinea, A., Playà, E., Rivero, L., Himi, M., 2010a. Electrical resistivity tomography and induced polarization techniques applied to the identification of gypsum rocks. Near Surf. Geophys. 8, 249–257.
Guinea, A., Playà, E., Rivero, L., Himi, M., Bosch, R., 2010b. Geoelectrical classification of gypsum rocks. Surv. Geophys. 31 (6), 557–580.
Guinea, A., Playà, E., Rivero, L., Ledo, J.J., Queralt, P., 2012. The electrical properties of calcium sulfate rocks from decametric to micrometric scale. J. Appl. Geophys. 85, 80–91.
Gutiérrez, F., Ortí, F., Gutiérrez, M., Pérez-González, A., Benito, G., Gracia, J., Durán Valsero, J.J., 2002. Paleosubsidence and active subsidence due to evaporite dissolution in Spain. Carbonates Evaporites 17 (2), 121–133.
Hashin, Z., Shtrikman, S., 1963. A variational approach to the theory of the elastic behavior of multiphase materials. J. Mech. Phys. Solids 11, 12–140.
Loke, M.H., 2002. RES2DMOD ver 3.0. 2D Resistivity and IP Forward Modelling. In: Loke Penang, M.H. (Ed.), .
Loke, M.H., Baker, R.H., 1996. Rapid least-squares inversion of apparent resistivity pseudosections by a quasi-Newton method. Geophys. Prospect. 44, 131–152.
Loke, M.H., Dahlin, T., 2002. A comparison of the Gauss–Newton and quasi-Newton methods in resistivity imaging inversion. J. Appl. Geophys. 49, 149–162.
Loke, M.H., Acworth, I., Dahlin, T., 2003. A comparison of smooth and blocky inversion methods in 2D electrical imaging surveys. Explor. Geophys. 34, 182–187.
Ma, Y., Wang, H., Xu, L.A., Jiang, C., 1997. Simulation study of the electrode array used in an ERT system. Chem. Eng. Sci. 52, 2197–2203.
Maillet, G.M., Rizzo, E., Revil, A., Vella, C., 2005. High resolution electrical resistivity tomography (ERT) in a transition zone environment: application for detailed internal architecture and infilling processes study of a Rhône River paleo-channel. Mar. Geophys. Res. 26, 317–328.
Ortí, F., 1997. Evaporitic sedimentation in the South Pyrenean Foredeeps and the Ebro basin during the tertiary: a general view. In: Busson, G., Schreiber, B.C. (Eds.), Sedimentary Deposition in Rift and Foreland Basins in France and Spain. Columbia University Press, New York, pp. 319–334.
Ortí, F., Salvany, J.M., 1997. Continental evaporitic sedimentation in the Ebro basin during the Miocene. In: Busson, G., Schreiber, B.C. (Eds.), Sedimentary Deposition in Rift and Foreland Basins in France and Spain. Columbia University Press, New York, pp. 420–429.
Ortí, F., Rosell, L., Anadon, P., 2010. Diagenetic gypsum related to sulfur deposits in evaporites (Libros Gypsum, Miocene, NE Spain). Sediment. Geol. 228, 304–318.
Salvany, J.M., 2009. Geología del yacimiento glauberítico de Montes de Torrero (Zaragoza). Prensas Universitarias de Zaragoza, p. 72.
Salvany, J.M., Ortí, F., 1987. La paragénesis de sulfatos de Ca y Na en el Mioceno continental de Alcanadre-Arrúbal (La Rioja) y San Adrián (Navarra). Bol. Soc. Esp. Mineral. 10 (1), 47–48.
Salvany, J.M., Ortí, F., 1994. Miocene glauberite deposits of Alcanadre, Ebro basin, Spain: sedimentary and diagenetic processes. In: Renaut, R.W., Last, W.M. (Eds.), Sedimentology and Geochemistry of Modern and Ancient Saline Lakes. , 50. SEPM Spec. Publ, pp. 203–216.
Salvany, J.M., Garcia-Veigas, J., Ortí, F., 2007. Glauberite–halite association of the Zaragoza Gypsum Formation (Lower Miocene, Ebro basin, NE, Spain). Sedimentology 54, 443–467.
Sasaki, Y., 1992. Resolution of resistivity tomography inferred from numerical simulation. Geophys. Prospect. 40, 453-46.
Shankland, T.J., Waff, H.S., 1977. Partial melting and electrical conductivity anomalies in the upper mantle. J. Geophys. Res. 82, 5409–5417.
Somerton, W.H., 1992. Thermal Properties and Temperature-related Behavior of Rock/Fluid Systems. Elsevier, Amsterdam (257 pp.).
Srinivasamoorthy, K., Sarma, V.S., Vasantavigar, M., Vijayaraghavan, K., Chidambaram, S., Rajivganthi, R., 2009. Electrical imaging techniques for groundwater pollution studies: a case study from Tamil Nadu state, South India. Earth Sci. Res. J. 13, 30–39.
Sumanovac, F., Dominkovic, S., 2007. Determination of resolution limits of electrical tomography on the block model in a homogenous environment by means of electrical modelling. Rudarsko-Geolosko-Naftni Zbornik, 19, pp. 47–56.
Szalai, S., Szarka, L., 2008. On the classification of surface geoelectric arrays. Geophys. Prospect. 56, 159–175.
Szalai, S., Novák, A., Szarka, L., 2009. Depth of investigation and vertical resolution of surface geoelectric arrays. J. Environ. Eng. Geophys. 14, 15–23.
Torquato, S., 2002. Random Heterogeneous Materials: Microstructure and Macroscopic Properties. Springer, p. 703.
Warren, J.K., 2006. Evaporites: Sediments, Resources and Hydrocarbons. Springer, p. 1035.
Warren, J.E., Price, A.C., 1961. Flow in heterogeneous porous media. Soc. Petrol. Eng. J. 1, 153–169.